ISSN 0252-1075
Contribution from IITM
Research Report No. RR-106

Simulation of Tropical Indian Ocean Surface Circulation Using a Free Surface Sigma Coordinate Model

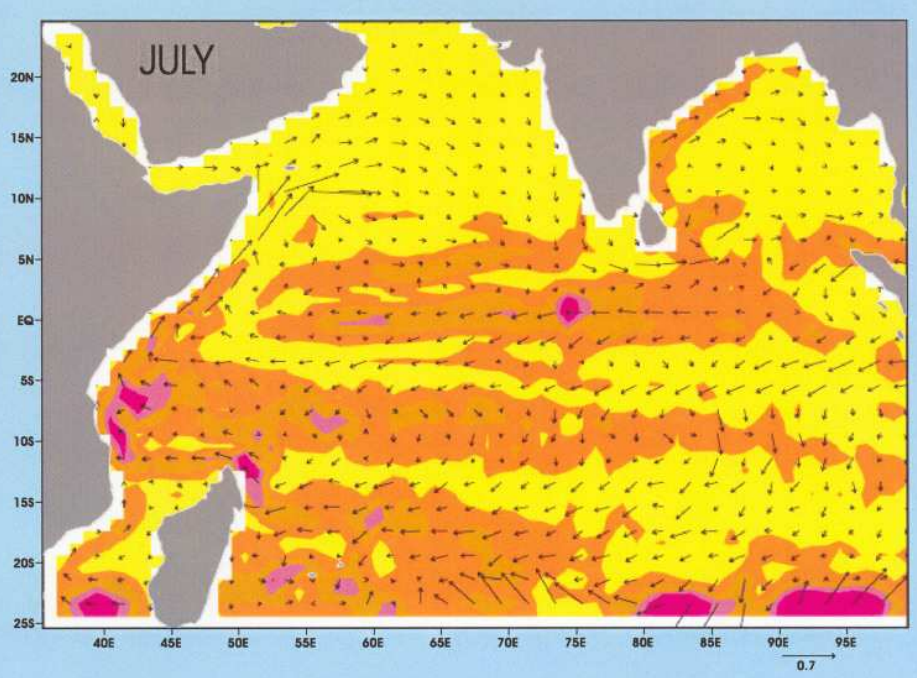

Prem Singh
and
P.S. Salvekar

December 2004

Indian Institute of Tropical Meteorology
Pune - 411 008, India

ISSN 0252-1075
Contribution from IITM
Research Report No. RR-106

Simulation of Tropical Indian Ocean Surface Circulation Using a Free Surface Sigma Coordinate Model

Prem Singh
and
P.S. Salvekar

December 2004

Indian Institute of Tropical Meteorology
Dr. Homi Bhabha Road, Pashan Pune - 411 008
Maharashtra, India

E-mail : lip@tropmet.res.in
Web : http://www.tropmet.res.in
Fax : 91-020-25893825
Telephone : 91-020-25893600

CONTENTS

Simulation of Tropical Indian Ocean Surface Circulation

Using a Free Surface Sigma Coordinate Model

Prem Singh* and P. S. Salvekar

Indian Institute of Tropical Meteorology, Pune-411008

ABSTRACT

In the present study the surface circulations in the Tropical Indian Ocean, obtained from the numerical experiments with a free surface sigma coordinate multi level ocean model commonly known as POM (Princeton University Ocean Model) are presented. This model has been originally developed for estuarian and coastal studies and due to large enhancement of computational power, only recently it has been applied to climatological problems. The model domain (35.5°E-99.5°E; 25.5°S-24.5°N) comprises the Arabian Sea, Bay of Bengal, and Tropical Indian Ocean. The horizontal resolution is 1°X1° latitude/longitude and vertical 21 levels of sigma coordinates from surface to bottom of the ocean are considered. The model is spun up for 16 years to reach quasi steady state. The monthly surface circulation from the model simulated steady state response is discussed.

Author's email address: psg@tropmet.res.in

1 Introduction

Ocean forms a vital component of the climate system. Ocean currents move large volume of warm and cold water around the globe. The surface circulations play an important role in the exchange of mass, momentum and energy between the atmosphere and ocean, so the circulation has an important effect on the climate. The Indian Ocean is unique in that it is limited in the north by the Asian continent. One consequence of this is that the Arabian Sea is forced by intense, seasonally reversing monsoon winds. These strong winds force the ocean locally, and they excite propagating signals (Kelvin and Rossby waves) that travel large distances and affect the ocean remotely. Thus, with such extraordinary phenomena as the Somali current, the equatorial jets and others (Tomczak and Godfrey, 1994), the Indian Ocean is an ideal " laboratory " for oceanographers, involving coastal, equatorial and subtropical ocean circulations, and the interactions between them.

Numerical ocean models and coupled ocean – atmosphere models (e.g. Delworth et al. 1993), developed in recent years, are major tools used to study interannual and interdecadal climate variabilities. Most of the previous simulations of the Tropical Indian Ocean, were based on Bryan-Cox model developed at the Geophysical Fluid Dynamics Laboratory or one and half layer reduced gravity model. The basin scale 1½ layer reduced gravity ocean model has been proven to simulate realistic observed surface currents on both monthly and seasonal scales as seen by Behera and Salvekar (1996, 1998). Isopycnal ocean models have also been used for large-scale simulations of Atlantic Ocean (Oberhuber, 1993). Another type of model used, is the free surface, bottom following sigma coordinate Princeton Ocean Model (POM), (Blumberg and Mellor, 1987), which has a turbulence closure scheme for surface and bottom mixed layer dynamics. This model was originally developed for estuarine and coastal studies and only recently has been applied to climatological problems. The understanding of the coastal circulation around India is very crucial for activities viz. navy, fishery, ocean biology, offshore exploration activities. In this study, POM model is used to simulate the surface circulation of Tropical Indian Ocean.

1.1 Observed features over Tropical Indian Ocean

The principal driving force for the surface currents in the Tropical Indian Ocean is the wind stress. The wind drives the ocean both directly and indirectly. Because of the Coriolis force, the direct forcing results in Ekman drift, by which wind driven current flows to the right of the wind direction in the Northern Hemisphere and to the left in the Southern Hemisphere. The coriolis parameter over the equator is zero so the current direction there tends to be directly down - wind. The reversal in the direction of the Ekman drift relative to the wind direction across the equator results in divergent flow away from the equator if wind is easterly, convergent if westerly; divergence leads to upwelling, convergence to downwelling. However, equatorial upwelling does not occur in the Indian Ocean as it does in the Pacific and Atlantic, because in

those oceans, upwelling occurs as a result of the south-east trade winds blowing across the equator and causing surface divergence. Since in the Indian Ocean, there is no such wind system in either season of the year, typical conditions for equatorial upwelling are missing. The wind affects currents indirectly in two ways, Firstly, the curl of the wind stress produces vertical motion in the oceanic boundary layer (so - called "Ekman Pumping"), this leads to vertical displacement of the thermocline, resulting in horizontal density gradients, which in turn produces geostrophic currents. Secondly, changes in the wind forcing can generate waves in the surface currents. These waves provide a key mechanism by which information can be transmitted rapidly within oceans. The equatorial region forms a wave guide for zonally propagating waves, enabling information to be carried out across a tropical ocean far more rapidly than at mid latitudes. Rossby waves are the principal mode for westward-propagating waves and Kelvin and Yanai (mixed Rossby–gravity) waves for eastward propagating disturbances.

1.2 Monsoon Currents

The monsoon currents extend over the entire basin from Somali coast to the eastern Bay of Bengal. Different parts of the currents form at different times and it is only in their mature phase that the currents exist as trans-basin flows. The westward winter monsoon current first forms south of Sri Lanka in November and is also fed by the equatorward East India Coastal Current (EICC). The westward winter monsoon current in the Southern Bay appears later. In its mature phase during December month, the winter monsoon current flows westward across the Southern Bay; it divides into two branches in the Arabian Sea. One of these branches continues flowing westwards, whereas the other turns around the Lakshdeep high (a sea-level high off southwest India) to flow into the poleward west India coastal current. The winter monsoon current is primarily a geostrophic current, modulated by Ekman drift.

Strong winds during the summer monsoon ensure that Ekman drift dominates at the surface, leading to a more complex vertical structure in the summer monsoon current than in winter monsoon current. The eastward flowing summer monsoon current first appears in the Southern Bay during May. In its mature phase, which peaks with the summer monsoon in July, the summer monsoon current in the Arabian Sea is a continuation of the Somali current and the coastal current off Oman. It flows eastward and south eastward across the Arabian Sea and around the Lakshdeep Low (a sea-level low off southwest India), eastward south of Sri Lanka and into the Bay of Bengal. The mature phase of the summer monsoon current lasts from May to September.

2 Brief Model Details

The POM model is a primitive equation model and it contains a second-order turbulence closure scheme providing the vertical mixing coefficients. The basic equations in sigma coordinates (Cartesian coordinates in horizontal) are

Continuity equation

$$\frac{\partial DU}{\partial x} + \frac{\partial DV}{\partial y} + \frac{\partial \omega}{\partial \sigma} + \frac{\partial \eta}{\partial t} = 0 \quad \text{.....(1)}$$

u momentum equation

$$\frac{\partial UD}{\partial t} + \frac{\partial U^2 D}{\partial x} + \frac{\partial UVD}{\partial y} + \frac{\partial U\omega}{\partial \sigma} - fVD + gD\frac{\partial \eta}{\partial x}$$
$$+ \frac{gD^2}{\rho_o}\int_\sigma^o \left[\frac{\partial \rho'}{\partial x} - \frac{\sigma'}{D}\frac{\partial D}{\partial x}\frac{\partial \rho'}{\partial \sigma'}\right] d\sigma' = \frac{\partial}{\partial \sigma}\left[\frac{K_M}{D}\frac{\partial U}{\partial \sigma}\right] + F_x \quad \text{..... .....(2)}$$

v momentum equation

$$\frac{\partial VD}{\partial t} + \frac{\partial UVD}{\partial x} + \frac{\partial V^2 D}{\partial y} + \frac{\partial V\omega}{\partial \sigma} + fUD + gD\frac{\partial \eta}{\partial y}$$
$$+ \frac{gD2}{\rho_o}\int_\sigma^o \left[\frac{\partial \rho'}{\partial y} - \frac{\sigma'}{D}\frac{\partial D}{\partial y}\frac{\partial \rho'}{\partial \sigma'}\right] d\sigma' = \frac{\partial}{\partial \sigma}\left[\frac{K_M}{D}\frac{\partial V}{\partial \sigma}\right] + F_y \quad \text{..... .....(3)}$$

temperature equation

$$\frac{\partial TD}{\partial t} + \frac{\partial TUD}{\partial x} + \frac{\partial TVD}{\partial y} + \frac{\partial T\omega}{\partial \sigma} = \frac{\partial}{\partial \sigma}\left[\frac{K_H}{D}\frac{\partial T}{\partial \sigma}\right] + F_T - \frac{\partial R}{\partial z} \quad \text{.....(4)}$$

salinity equation

$$\frac{\partial SD}{\partial t} + \frac{\partial SUD}{\partial x} + \frac{\partial SVD}{\partial y} + \frac{\partial S\omega}{\partial \sigma} = \frac{\partial}{\partial \sigma}\left[\frac{K_H}{D}\frac{\partial S}{\partial \sigma}\right] + F_S \quad \text{.....(5)}$$

Two more prognostic equations are used to calculate turbulence kinetic energy and turbulence lengthscale

$$\frac{\partial q^2 D}{\partial t} + \frac{\partial Uq^2 D}{\partial x} + \frac{\partial Vq^2 D}{\partial y} + \frac{\partial \omega q^2}{\partial \sigma} = \frac{\partial}{\partial \sigma}\left[\frac{K_q}{D}\frac{\partial q^2}{\partial \sigma}\right]$$
$$+ \frac{2K_M}{D}\left[\left(\frac{\partial U}{\partial \sigma}\right)^2 + \left(\frac{\partial V}{\partial \sigma}\right)^2\right] + \frac{2g}{\rho_o}K_H\frac{\partial \tilde{\rho}}{\partial \sigma} - \frac{2Dq^3}{B_1 l} + F_q \quad \text{. ....(6)}$$

$$\frac{\partial q^2 lD}{\partial t} + \frac{\partial Uq^2 lD}{\partial x} + \frac{\partial Vq^2 lD}{\partial y} + \frac{\partial \omega q^2 l}{\partial \sigma} = \frac{\partial}{\partial \sigma}\left[\frac{K_q}{D}\frac{\partial q^2 l}{\partial \sigma}\right]$$

$$+ E_1 l\left(\frac{K_M}{D}\left[\left(\frac{\partial U}{\partial \sigma}\right)^2 + \left(\frac{\partial V}{\partial \sigma}\right)^2\right] + E_3 \frac{g}{\rho_o} K_H \frac{\partial \rho}{\partial \sigma}\right) - \frac{Dq^3}{B_1}\tilde{W} + F_l \quad \text{.....(7)}$$

where σ	=	$(z-\eta)/(H+\eta)$; $D= \eta+H$;
$\eta(x, y, t)$	=	Free surface elevation
$H(x, y)$	=	water depth
T	=	temperature
S	=	salinity
ω	=	vertical velocity in sigma coordinate
U, V	=	zonal and meridional velocity
g	=	acceleration due to gravity
f	=	$2\Omega\sin\phi$ Coriolis parameter for latitude ϕ
A_M, K_M	=	horizontal and vertical kinematic viscosity
$A_H, K_H,$	=	horizontal and vertical diffusivity
Kq	=	turbulence mixing coefficient
q^2	=	turbulence kinetic energy
l	=	turbulence length scale
ρ	=	in situ density
ρ_0	=	reference density
c_s	=	speed of sound
F_q, F_l	=	horizontal mixing
E_1, E_3, B_1	=	constants
R	=	short wave radiation
$\tilde{W}$	=	$\{1+E_2(l/\kappa L)\}$ is wall proximity function where $L^{-1}=(\eta-z)^{-1} + (H-z)^{-1}$

$$\frac{\partial \tilde{\rho}}{\partial \sigma} = \frac{\partial \rho}{\partial \sigma} - c_s^{-2}\frac{\partial p}{\partial \sigma}$$

The horizontal viscosity and diffusion terms are defined according to:

$$F_x \equiv \frac{\partial}{\partial x}(H\tau_{xx}) + \frac{\partial}{\partial y}(H\tau_{xy})$$

$$F_y \equiv \frac{\partial}{\partial x}(H\tau_{xy}) + \frac{\partial}{\partial y}(H\tau_{yy})$$

where

$$\tau_{xx} = 2A_M\frac{\partial U}{\partial x},\quad \tau_{xy} = \tau_{yx} = A_M\left(\frac{\partial U}{\partial y} + \frac{\partial V}{\partial x}\right),\quad \tau_{yy} = 2A_M\frac{\partial V}{\partial y}$$

Also,

$$F_\phi \equiv \frac{\partial}{\partial x}\left(Hq_x\right) + \frac{\partial}{\partial y}\left(Hq_y\right) \quad \text{.....(8)}$$

where

$$q_x \equiv A_H \frac{\partial \phi}{\partial x}, \quad q_y \equiv A_H \frac{\partial \phi}{\partial y} \quad \text{.....(9)}$$

and where ϕ represents T, S, q^2 or $q^2 l$

The vertical mixing coefficients K_M and K_H in equations (2), (3), (4), (5) are obtained by using a second order turbulence closure scheme (Mellor and Yamada 1974).

3 Model Setting and Methodology

The model assumes rectangular coordinate in the horizontal having resolution 1°X°1 lat/lon. The model domain covers 25.5°S to 24.5°N and 35.5°E to 99.5°E. The model uses the Arakawa 'C' grid finite differencing scheme. The model has realistic coastline and topography based on ETOPO5 data set and is shown in fig.1. As it is known that surface circulation is mainly dominated by surface winds, the input forcings used in the model are monthly mean surface wind stress for years 1980-1989 from ECMWF analyses (Trenberth et. al. 1989) as surface forcing, and annual mean temperature and salinity from Levitus climatology (1994) is used as internal forcing. The wind stress is available for 2.5°X2.5°lat/lon resolution and is interpolated by using cubic spline technique for the model grid and is shown in fig.2 and Fig.3. The north easterly winds are dominated over the model region north of equator during November to March with maximum value of wind stress in January. The intense southwesterly winds dominate during the month of May to September with maximum values in July-August. South of equator, windstress is northwestward with its maximum intensity in July. The annual mean temperature and salinity data is available for Z = 0 to Z = 5500 meter depth is also interpolated by using cubic spline technique for the vertical model grid.

There are 21 σ levels in the vertical between $\sigma = 0$ and $\sigma = -1$ where $\sigma = (z-\eta) / (H+\eta)$, $\eta(x,y)$ and $H(x,y)$ are the surface elevation and water depth. The vertical resolution is higher near the surface and lower near the bottom. The horizontal time differencing scheme is explicit, whereas vertical time differencing scheme is implicit. The model has a split time step; a two dimensional external mode that uses a short time step of 60 seconds and a three dimensional internal mode time step of 1800 seconds. We assume that the monthly mean wind data represents the value at middle of representative month and then linearly interpolated to get input at model time steps. The model integration is carried out for 16 years to reach quasi steady state. Results of the steady state response are discussed below.

4 Results and Discussion

The aim of the present study is to determine the effect of wind forcing on monthly surface circulation in the model domain. Further, the seasonal cycle of surface circulation is also examined. The model simulation of the seasonal cycle is compared with estimates of current climatology from observations. The schematic surface circulation of Tropical Indian Ocean is shown in fig.4 for winter and summer seasons. The current climatologies used are those given by Hastenrath (1985) and an analysis by Rao et al (1989) of the ship-drift data-set produced by Cutler and Swallow (1984) are shown in fig.5. The principal features of the Indian Ocean circulation are well reproduced by the model in response to forcing by seasonally varying climatological winds.

The main features in the summer season are Somali Current (SC), South West Monsoon Current, South Equatorial current etc. and in the winter season North Equatorial current, Equatorial counter current, South Equatorial current, East India Coastal Current (EICC), West India Coastal Current (WICC). On account of the seasonal reversal of the wind on the northern part of Indian Ocean, the general scheme of its surface circulation differs from winter to summer. From November to March i.e. NE Monsoon, the winds blow from the north – east and during May to September i.e. SW Monsoon, the wind blow from the southwest. The change of wind direction north of equator then results in a change of surface current. The month wise simulated currents are presented in Fig.6 to Fig.11 and are discussed with reference to the observed climatological features of the Tropical Indian Ocean.

4.1 Equatorial Currents

South Equatorial Current

A broad westward flowing SEC is seen in most of the climatological charts between 8°S and 20° S almost throughout the year. The westward flowing currents (SEC) between 10°S and 20° S can be generally seen almost throughout the year in the model simulation.

North Equatorial current and Somali Current

The model produced NEC is seen to change the direction four times in a year flowing eastward during summer monsoon. The January and February (Fig.6) charts show the northeast monsoon situation. At this time of the year the wind field mostly resembles the trade wind systems of the other two oceans. There is generally a westward flow of the northeast monsoon current in the Northern Hemisphere extending up to 2°S. It deflects into moderate, generally southwestward current along the Somali coast. An eastward equatorial counter current exist in the Southern Hemisphere between 2S° to 8°S.

In April the establishment of strong eastward jet within few degrees of equator in the central and eastern part of the Indian Ocean. This arises as direct response to the moderate equatorial westerlies as noted by Wyrtki (1973). The strong ocean response to these moderate winds is due to weak coriolis force.

During boreal winter the winds are northeasterly in the north Indian Ocean and the Somali current along the Somali coast flows southward. This is seen in the model simulated January circulation. The flow is from 5°N to equator in November and the flow is moved further south till 5°S in January (Fig.6). These features are in qualitative agreement with the observed climatological atlases Duing (1970), Wyrtki (1971) Hasternath and Greischar (1989), Rao et al (1991) and the model results of Luther and O'Brien (1989), Woodbery et al (1989). During spring season (prior to SW monsoon) the surface current along Somali coast starts flowing northward. The model results suggest northward flow north of 5°N in March and northward along the coast in April. This is in good agreement with the results reported by Schott and Quadfasel (1982). As the southward flowing Somali current disappears in April and wind starts blowing southward, the East African coastal current reaches equator. An anticyclonic gyre south of the equator is simulated in winter season (Fig11 and Fig.1). This gyre forms when Somali current that flows southward joins the northward flowing East African coastal Current (EACC). The southward flowing Somali Current in the winter months (Nov, Dec, Jan) disappears in March (Fig.7).

With the onset of the South -West monsoon an anti cyclonic gyre, the great whirl develops from 4°N-10°N by June (Fig.8), which persists throughout the monsoon. In the late phase of monsoon, the Great whirl has become an almost closed circulation cell in Aug. and Sep. (Fig.8 and Fig.9). In summer by July and August, the fully developed southwest monsoon drives the eastward flow in the northern ocean. This is called as monsoon current. This feature is clearly simulated in the present study. The North equatorial current, seen in the winter season disappears and equatorial counter current moves in north of the equator. This fact is clearly simulated in the present study. The model SEC flows directly to the east coast of Madagascar as the model geometry does not include the small island east of Madagascar. It splits near Madagascar coast near 17°S which is in agreement with observation (Schott et. al. 1988). One branch flows south and the other flows north. The northward branch again splits at the African coast and the northward flowing part feeds EACC and the southward flowing part is known as Mozambique current.

4.2 Bay of Bengal

As in the case of Somali Current the East India Coastal Current (EICC) also reverses direction twice a year flowing North Eastward from February until September with a strong peak in March-April and southwestward from October to January with strongest flow in November. Large basin wide anticyclonic gyre in winter and spring i.e. December to April is seen in the Bay, which agree very well with model studies of Potemra (1991). The gyre has northward flow along east coast north of 15°N in December (Fig.11) and all along east coast in the other months (Jan-April). During summer months, northward flow along east coast is in agreement with the ship drift observation.

4.3 West Indian Coastal Current

The circulation in the interior Arabian is mostly in Sverdrup balance throughout the year i.e. the flow is southward in summer and northward in winter. The circulation features along west coast of India are opposite to that of the wind direction. Cutler and Swallow (1984) ; Shetye and Shenoy (1988) using the ship drift observations suggested a southward flow that appears along the west coast of India in March, reaches a maximum in July and vanishes by October. This is called the West India Coastal Current WICC and it changes its direction seasonally. This feature is clearly seen in fig. 8 and fig.11.

WICC flows northward during the winter monsoon (fig.10 and fig.11). The ship-drift currents indicated that the northward WICC at this time is the strongest west coastal current throughout the year, and yet the coastal winds are very weak or absent at this time. This property lends strong support for the importance of remote forcing.

5 Conclusions

This study examines the seasonal cycle of surface circulations in the Tropical Indian Ocean as simulated by a 3-D ocean model. The ocean currents in the Tropical Indian Ocean are primarily driven by the seasonally reversing monsoonal circulations, which make them different from circulation patterns in the Pacific and Atlantic oceans. The main features of the Tropical Indian Ocean circulation (South Equatorial Current, North Equatorial current and Somali Current, Bay of Bengal, West Indian Coastal Current) are found to be well simulated by the model. The interannual variability in the upper layer circulation as simulated by POM model will be addressed in the next part of the study.

Acknowledgements

Authors are thankful to the Director, IITM for encouragement and support. Thanks are due to Dr. Bryan Doty of COLA for kindly providing the GrADS software that was used in the preparation of the figures. Authors are thankful to Dr. R. Krishnan for fruitful suggestions in the improvement of the manuscript. This work was carried out in the PIV desktop machine using Linux environment.

References

1. Blumberg, A.F. and Mellor, G.L., A description of a three-dimensional coastal circulation model, in Three-Dimensional Coastal ocean Models, Coastal Estuarine Ser., vol. 4, edited by N. S. Heaps. 208 pp., Agu, Washington, D.C., 1987.

2. Behera, S.K. and Salvekar, P.S., Development of Simple reduced gravity ocean model for the study of upper North Indian Ocean IITM Research Report, RR 072, 1996.

3. Behera, S.K. and Salvekar, P.S., Numerical Investigation of coastal circulation around India Mausam, 49, 345-360, 1998.

4. Cutler, A.N. and Swallow, L.C., Surface currents of the Indian Ocean (to 25°S, 100°E); compiled from historical data archived by the Meteorological Office, Bracknell, UK. I.O.S., Wormley, UK, Report No. 187, 1984.

5. Delworth,T., Manabe, S. and Stouffer, R.J., Interdecadal variations of the thermohaline circulation in a coupled ocean-atmosphere model, J. Clim., 6, 1993-2011, 1993.

6. Duing, W., *The monsoon regime of the currents in the Indian Ocean*, East-West Center Press, Honolulu, 68pp., 1970.

7. Hasternath, S and Greischar, L. Climate atlas of the Indian Ocean, Part-III, Upper ocean structure, The University of Wisconsin Press, 247 charts, 1989.

8. Hastenrath, S., *Climate and Circulation of the Tropics*. D.Reidel Publishing Co., 455pp., 1985.

9. Levitus S., Burgett, R. and Boyer, T.P., World Ocean Atlas 1994 Volume 3, Salinity. NOAA Atlas NESDIS 3, U.S. Department of Commerce, Washington, D.C. 99 pp., 1994.

10. Levitus S. and Boyer, T.P., World Ocean Atlas 1994 Volume 4, Temperature. NOAA Atlas NESDIS 4. U.S. Department of Commerce, Washington, D.C. 117 pp., 1994.

11. Luther, M.E and O'Brien, J.J., Modelling the variability in Somali Current, Meso scale/Synoptic coherent structure in Geophysical Turbulence ; Eds J.C.J. Nihoul and B.M. Jamart, Elsevier Science Publ. 373-386, 1989.

12 Mellor, G.L., and Yamada, T., A hierarchy of turbulence closure models for planetary boundary layers, J. Atmos. Sci., 31, 1791-1806, 1974.

13. Oberhuber, J.M., Simulation of the Atlantic circulation with a coupled sea ice-mixed layer-isopycnal general circulation model, II, Model experiment, J. Phys. Oceanogr., 23, 830-845, 1993.

14. Potemra. J.T., Luther, M.E and O'Brien, J.J., The Seasonal circulation of the upper Ocean in the Bay of Bengal. J.Geophy. Res., 96, 12667-126683, 1991

15. Rao, R.R, Molinari, R.L., and Festa, J.F., Surface meteorological and near surface oceanographic atlas of the tropical Indian Ocean, NOAA Technical Memorandum, ERLAOML-69, 1991.

16. Rao, R. R., Molinari, R. L. and Festa, J.F., Evolution of the climatological near- mixed layer depth, and sea surface temperature, surface current, and surface meteoro logical fields, *J. Geophys. Res.*, 94, 10801–10815, 1989.

17. Reddy P. Rahul Chand, Salvekar, P.S., Ganer, D.W. and Deo, A.A., Evidence of twin gyres in the Indian Ocean : New insight using reduced gravity model forced by daily winds, IITM Research Report-096, 1996.

18. Schott F. and Quadfasel D.R., Variability of the Somali current system during the onset of the southwest monsoon. J. Phys. Ocn. 12, 1343-1357, 1982.

19. Schott F., Fieux, M., Kindle, J., Swallow, J. C., and Zantopp, R., The boundary currents east and north of Madagascar, Direct measurements and model comparison, J.Geophys. Res., 93, 4963-4974, 1988.

20. Shankar, D., Vinayachandran, P. N., Unnikrishnan, A. S., and Shetye, S. R., The monsoon currents in the north Indian Ocean, Progress in Oceanography., vol 52(1), 63-119, 2002

21.Shetye S.R., and Shenoi, S.S.C., The seasonal cycle of surface circulation in the coastal north Indian Ocean, Proceeding of the Indian Academy of Sciences 93 (4) 399-411, 1988.

22. Trenberth, K.E., Olson, J.G. and Large, W.G., A global ocean wind stress climatology based on ECMWF analyses. NCAR Tech. Note NCAR/TN-338+STR, 93 pp., 1989

23. Tomczak, M. and Godfrey, J.S., *Regional Oceanography : An Introduction.* Pergamon. Pp. 422., 1994

24. Woodberry, K.E., Luther, M.E and O'Brien, J.J., The wind driven seasonal circulation in the southern tropical Indian Ocean , J. Geophys. Res., 94, 17, 985-18,002, 1989.

25. Wyrtki.K., An equatorial jet in the Indian Ocean, Science, 181,262-264, 1973.

26.Wyrtki.K., Oceanographic atlas of the International Indian Ocean Expedition, National Science Foundation , Washington, D.C. 531pp, 1971.

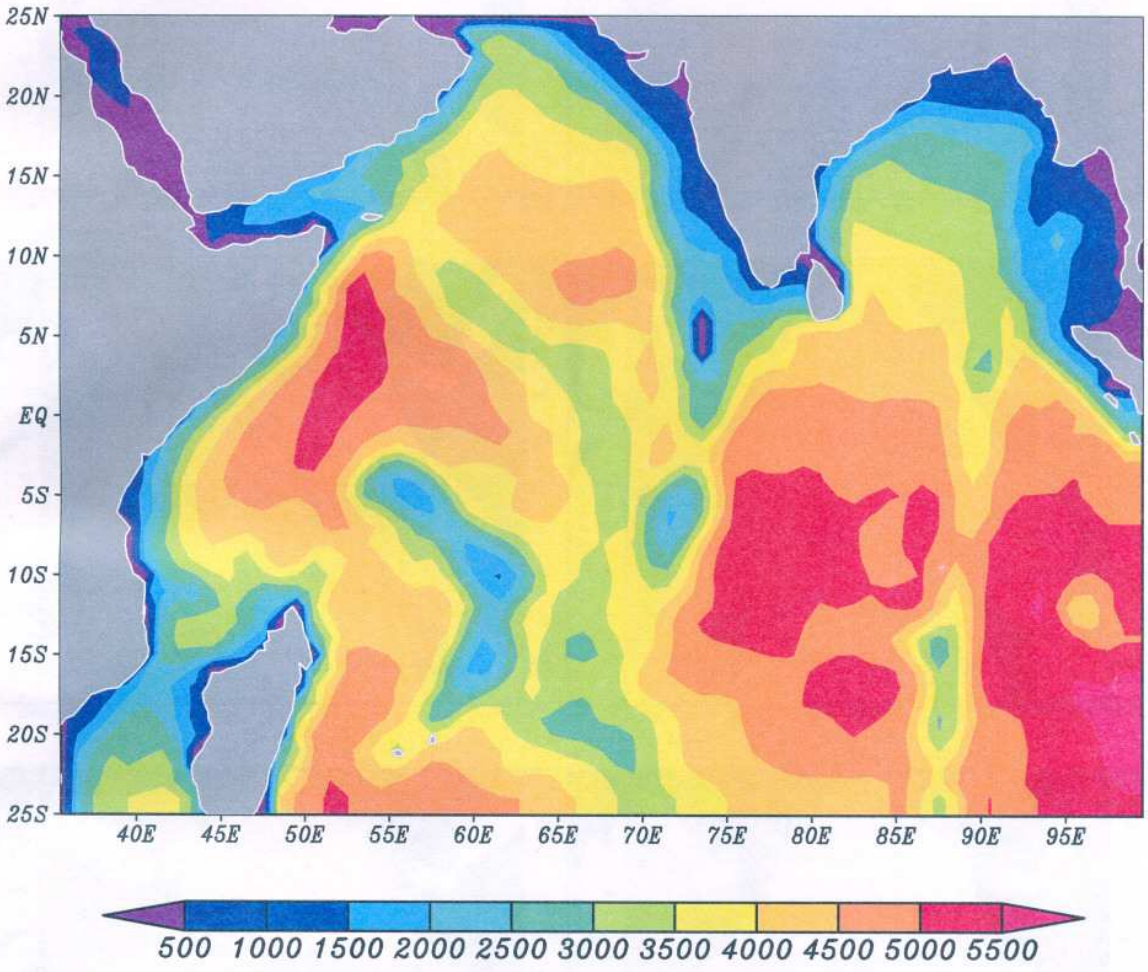

Fig. 1 Water depth (meters)

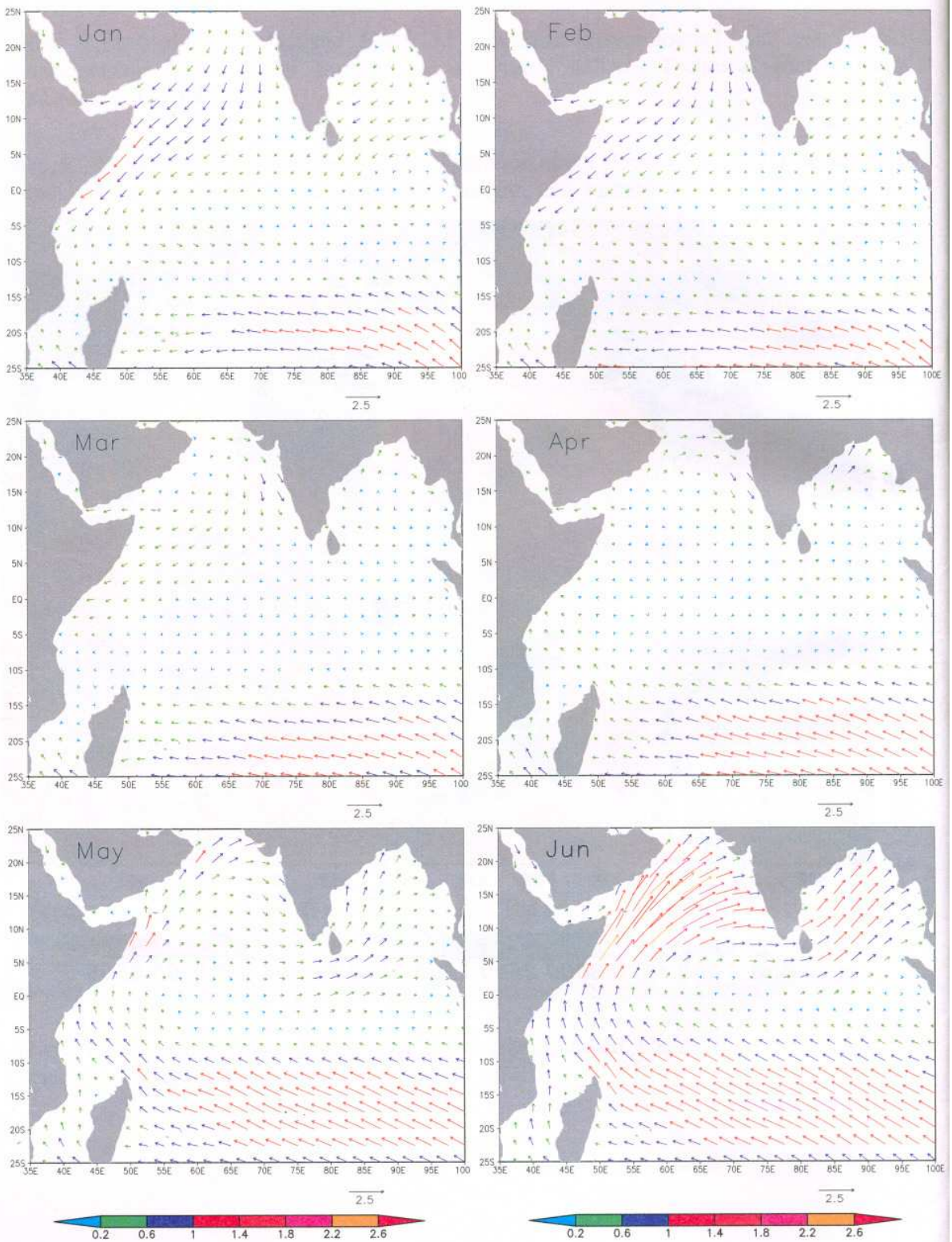

Fig. 2 Surface Wind stress from Jan to Jun (dynes/cm**2)

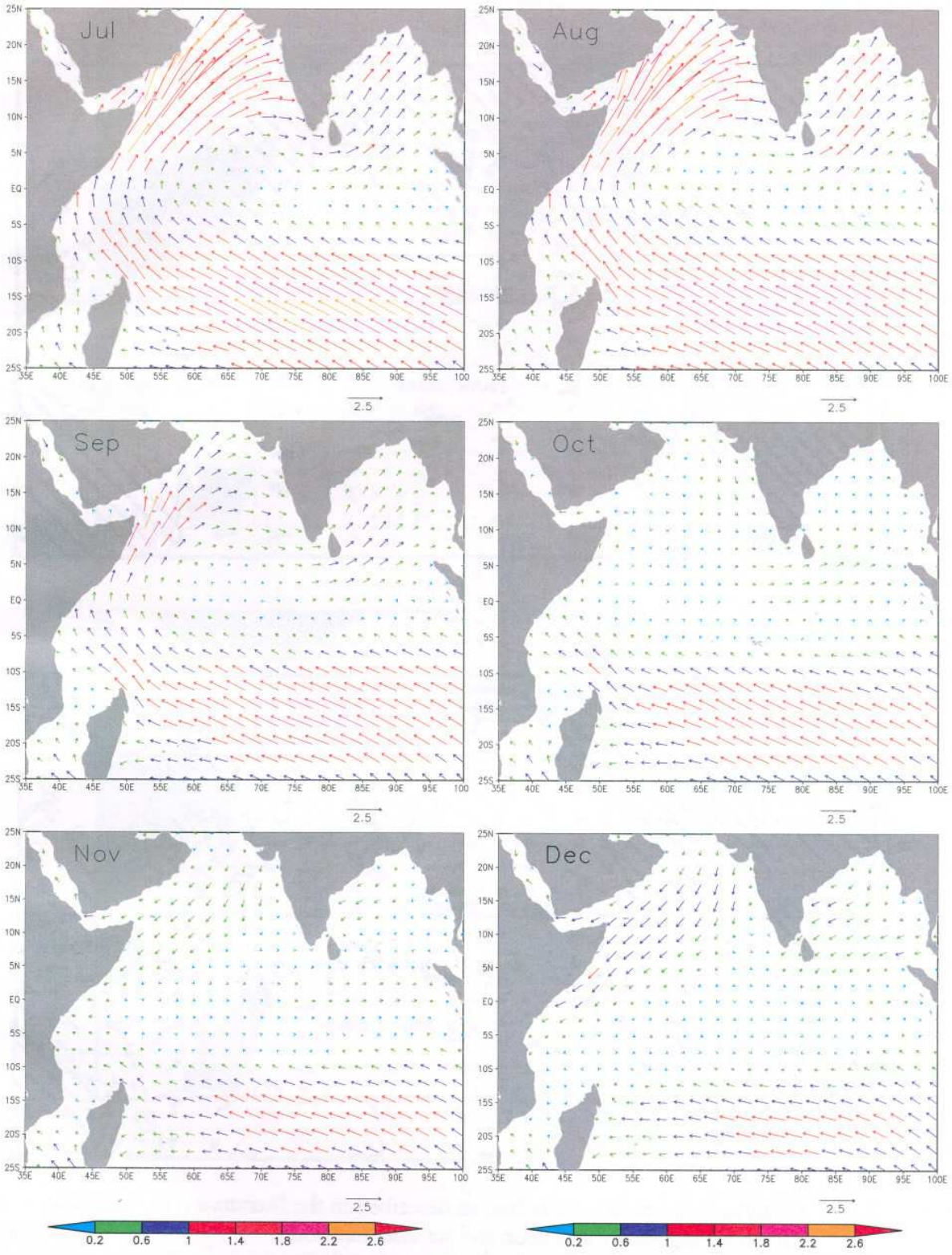

Fig. 3 Surface Wind stress from Jul to Dec (dynes/cm**2)

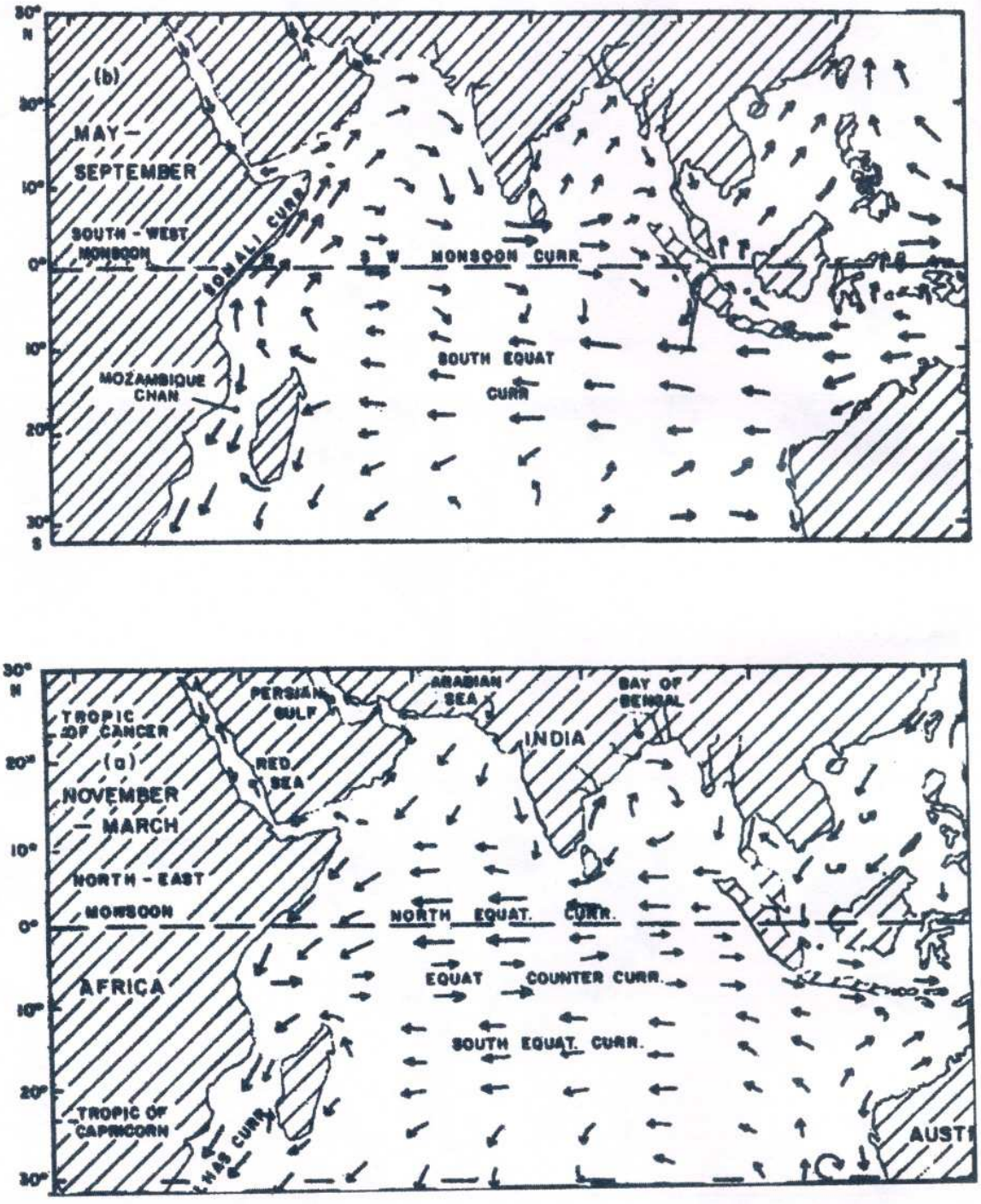

Fig. 4 Observed surface of circulation, as described in the literature , in the Indian Ocean during winter monsoon and summer monsoon.

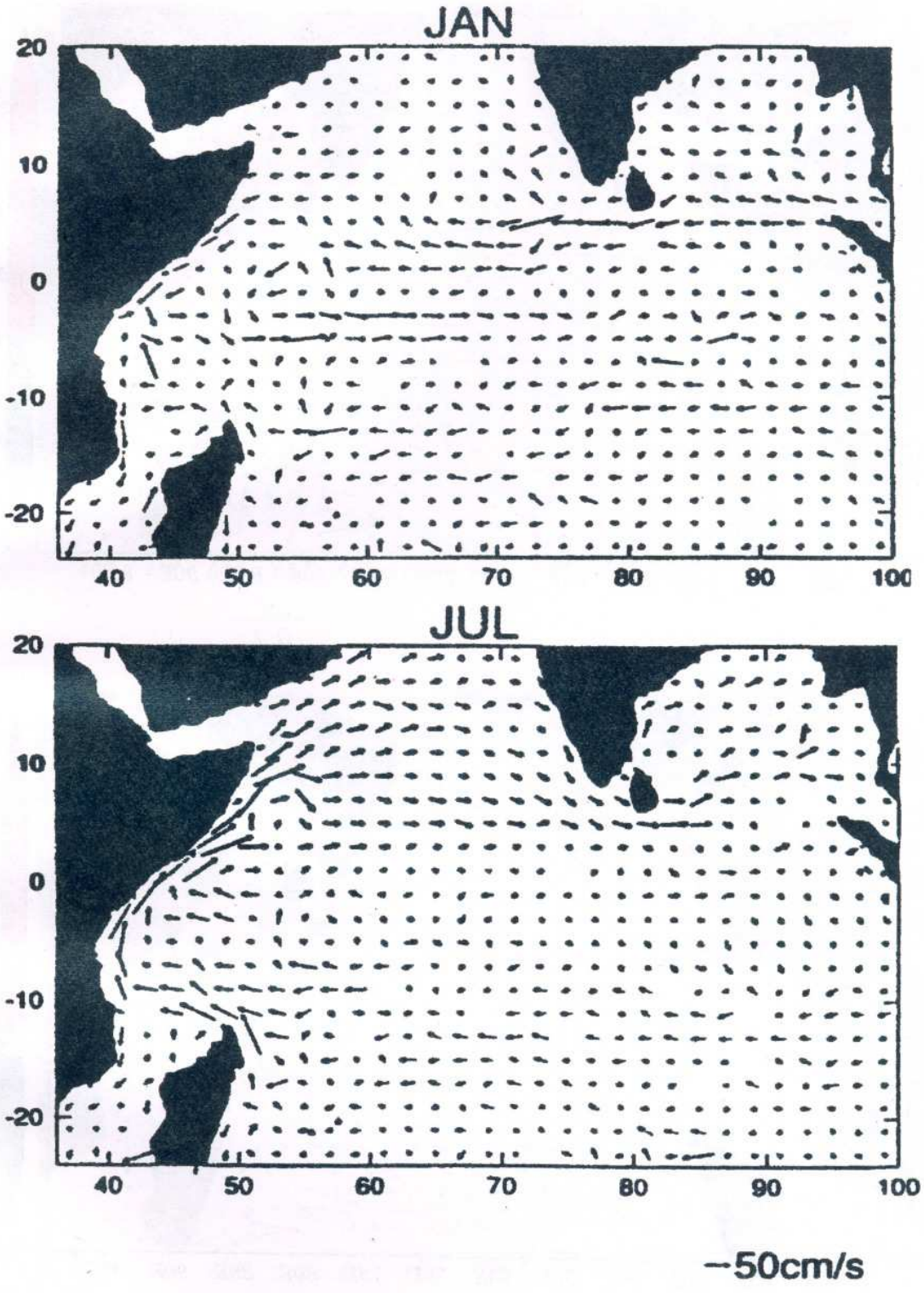

Fig. 5. Observed mean monthly ship drift currents for January and July from analysis by Rao et al (1989) of ship drift climatology of Cutler and Shallow (1984)

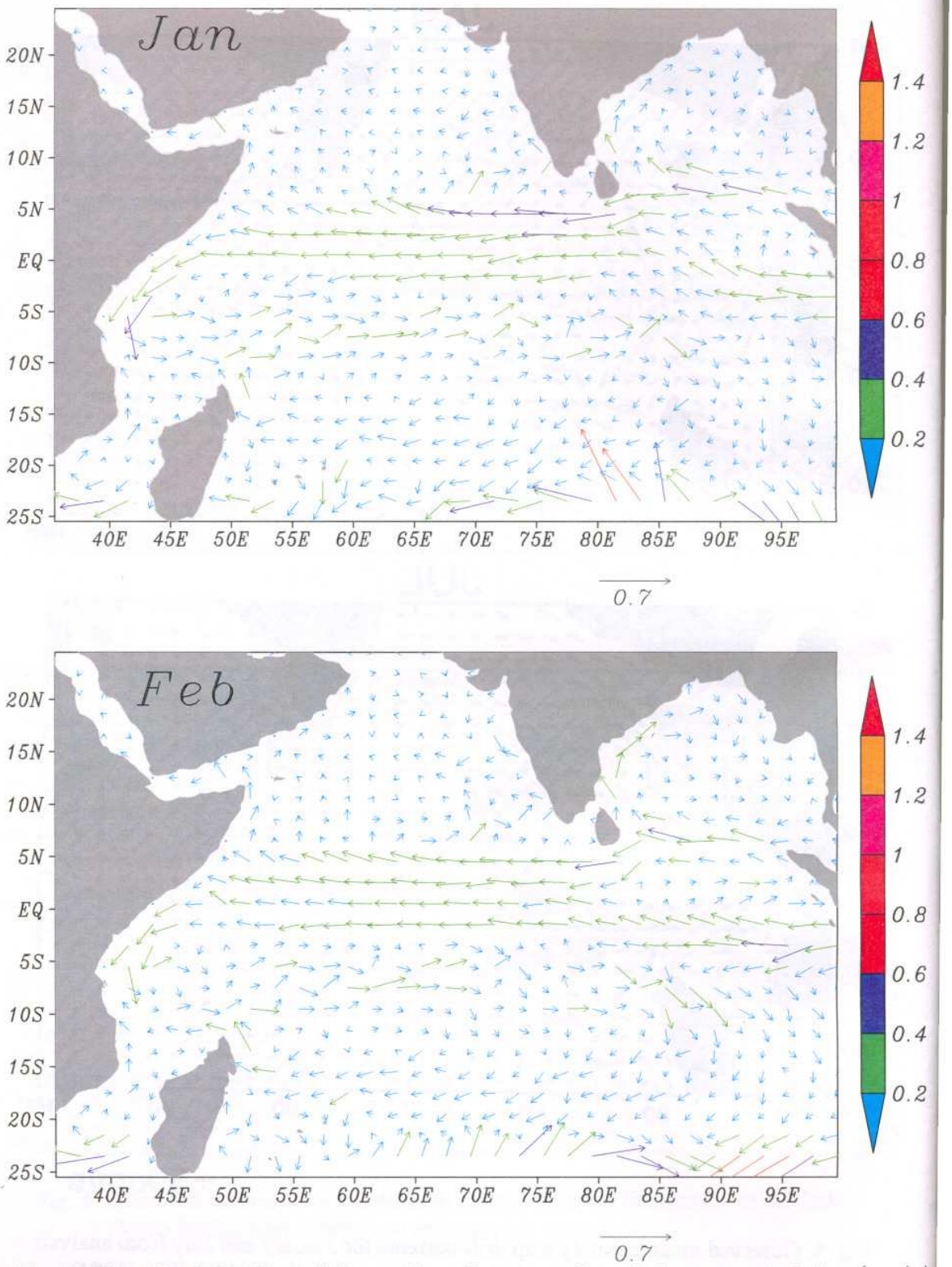

Fig.6 The Model Climatology for the month of Jan. and Feb. (m/s)

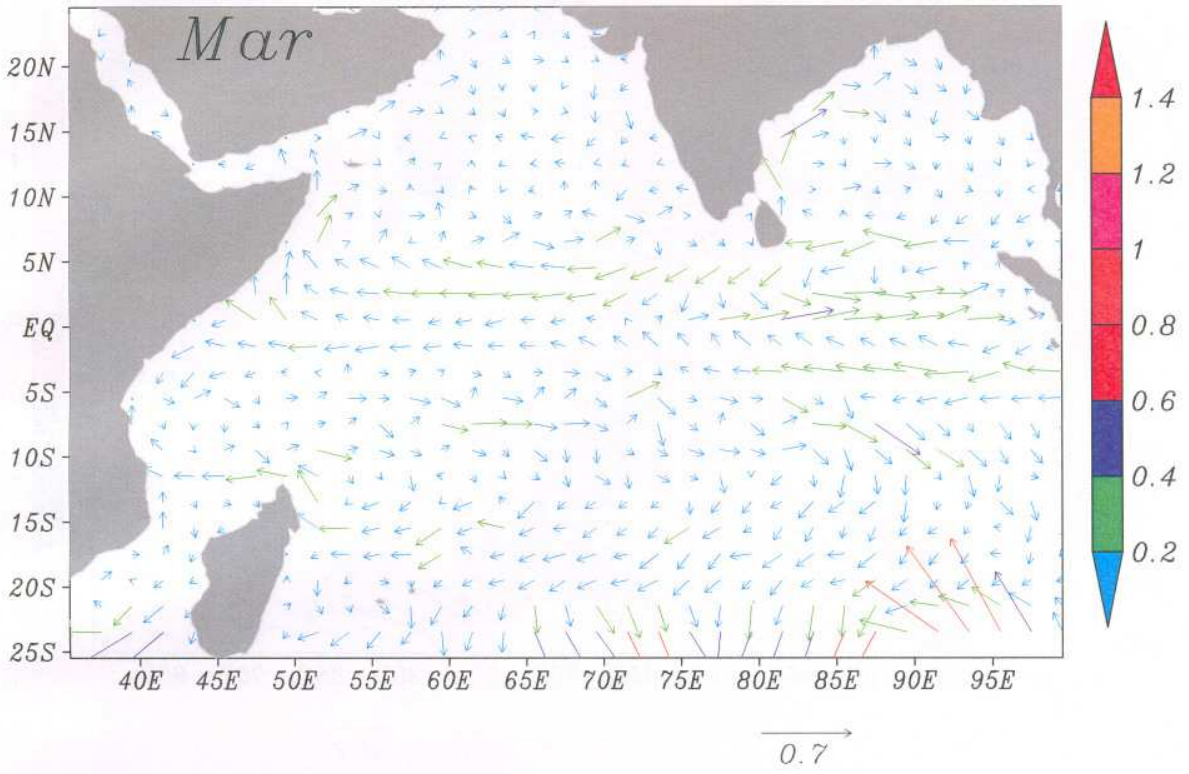

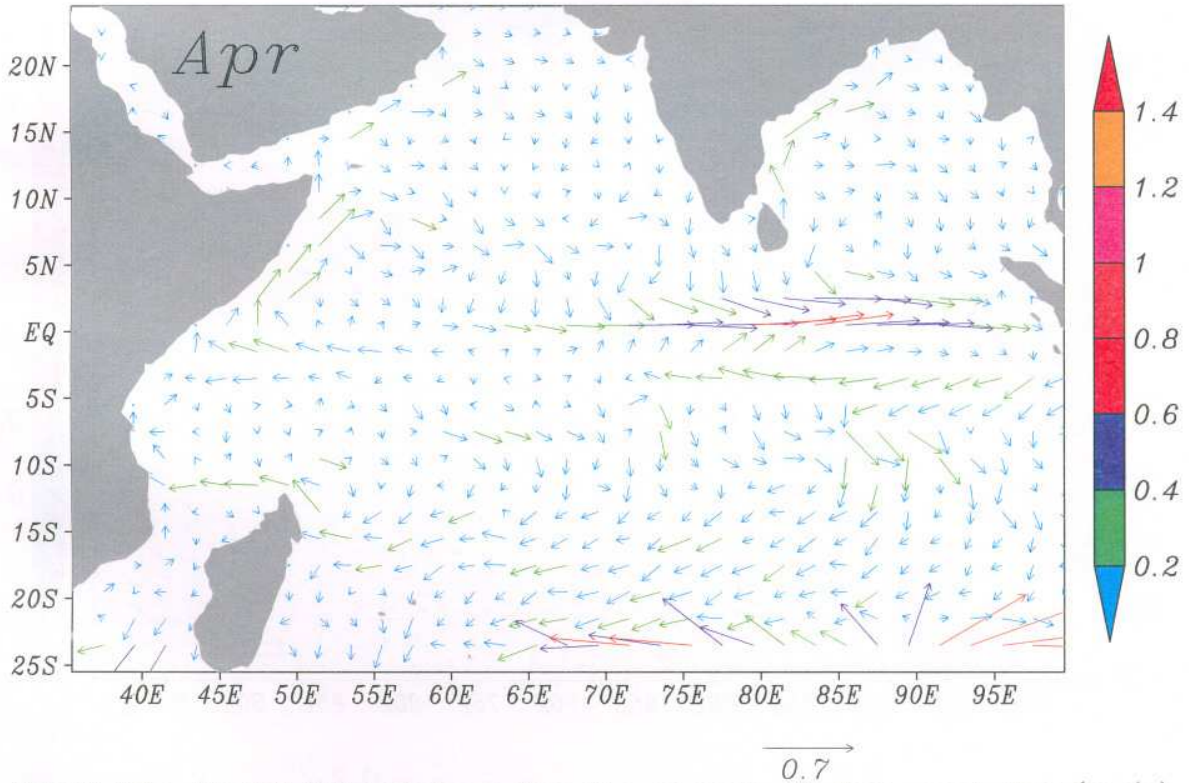

Fig.7 The Model Climatology for the month of Mar. and Apr.(m/s)

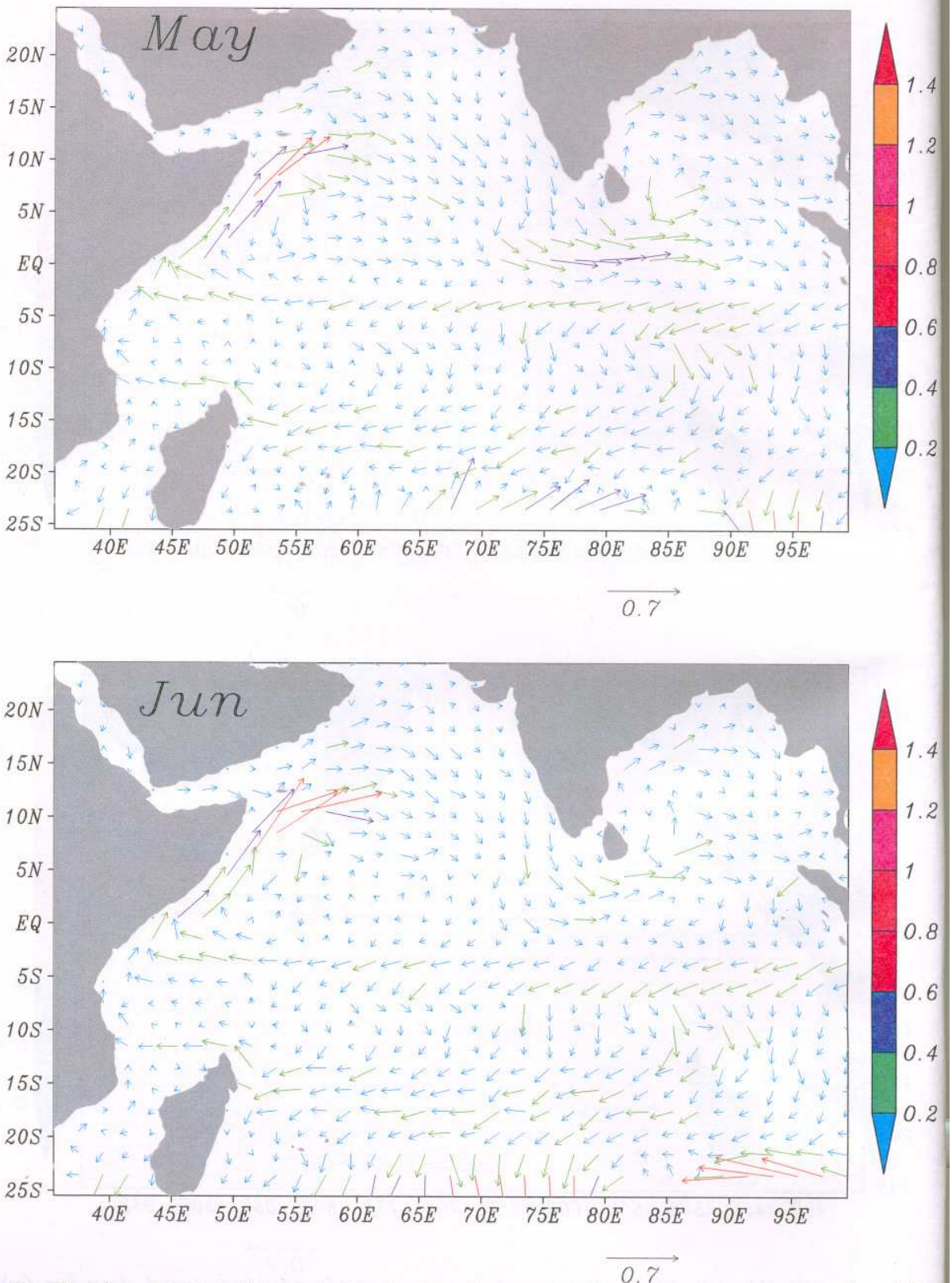

Fig.8 The Model Climatology for the month of May and Jun(m/s)

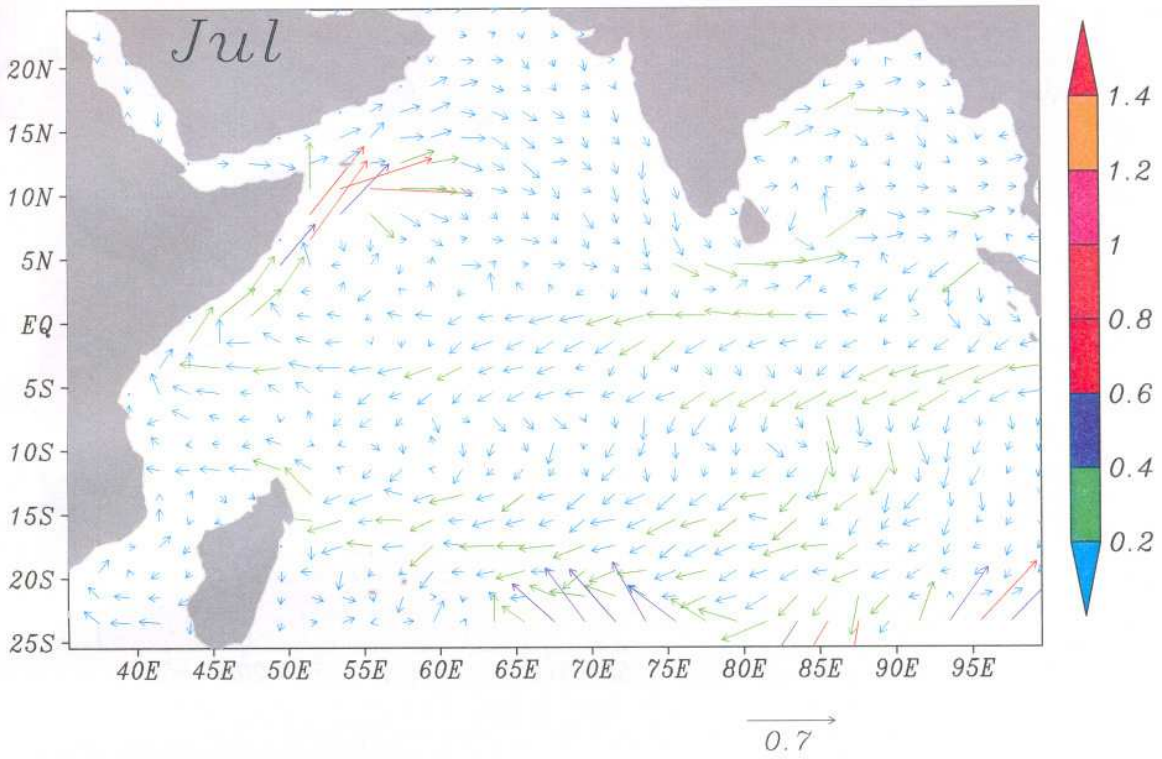

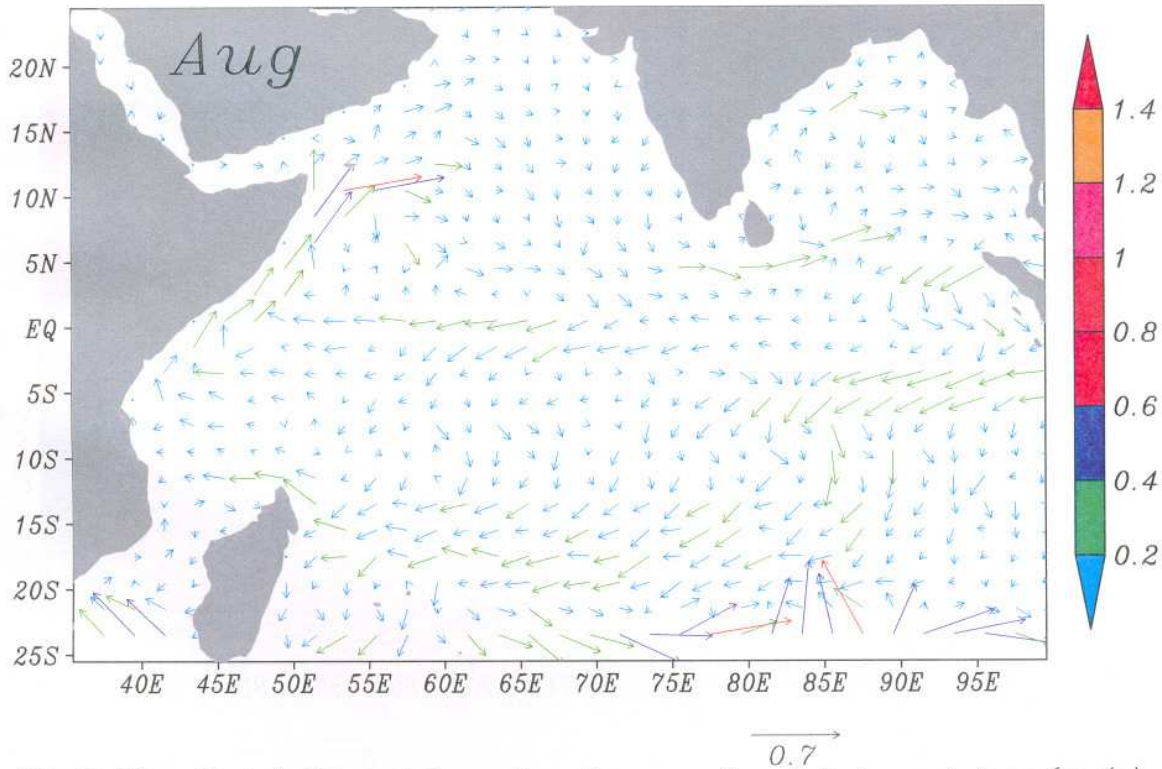

Fig.9 The Model Climatology for the month of Jul. and Aug.(m/s)

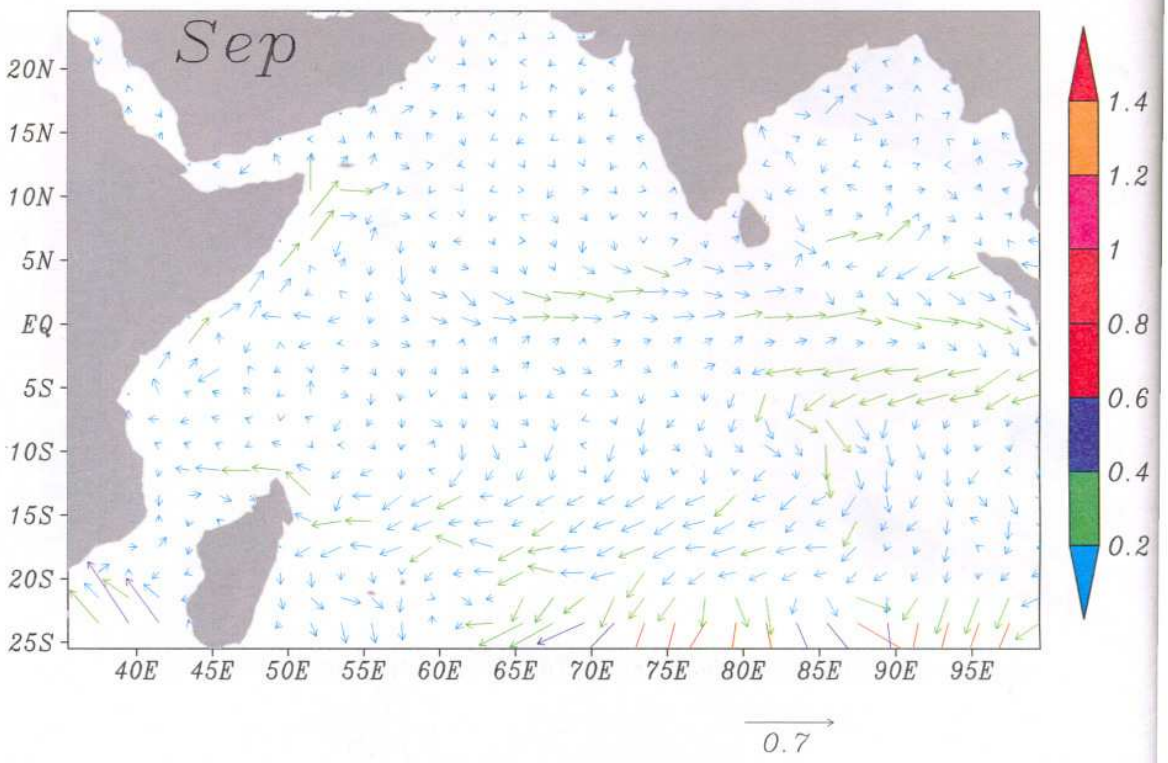

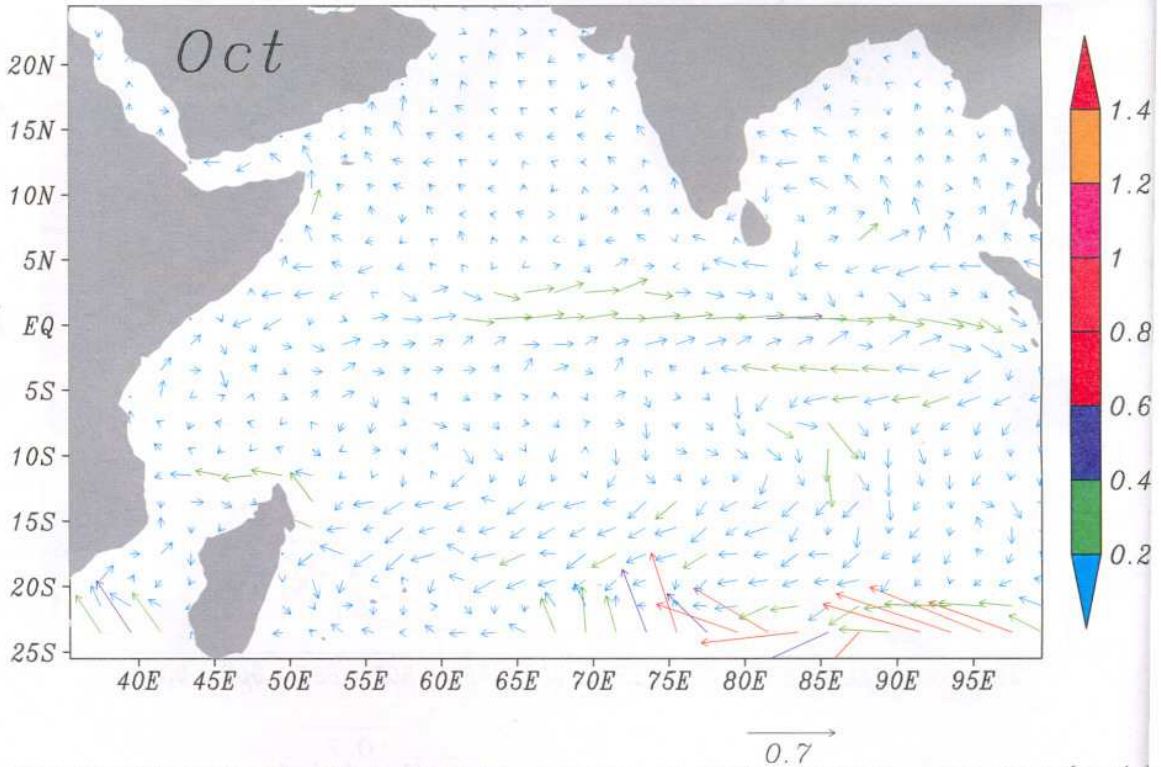

Fig.10 The Model Climatology for the month of Sep. and Oct.(m/s)

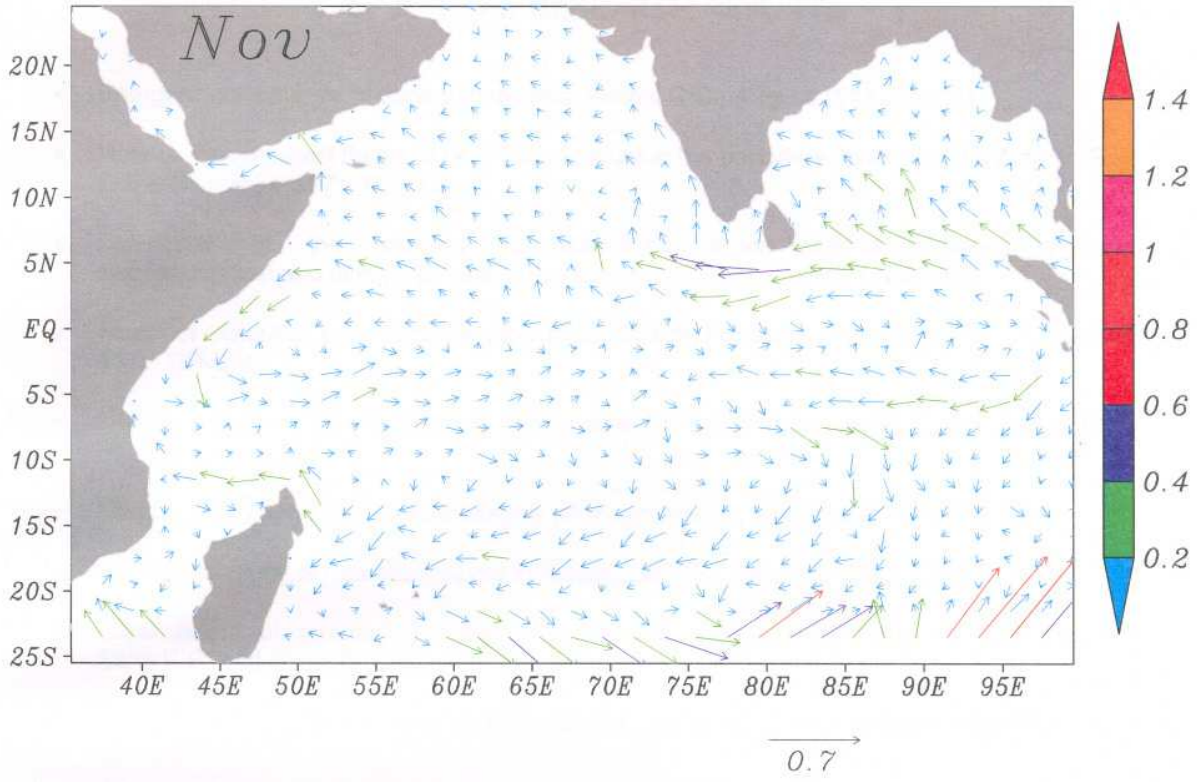

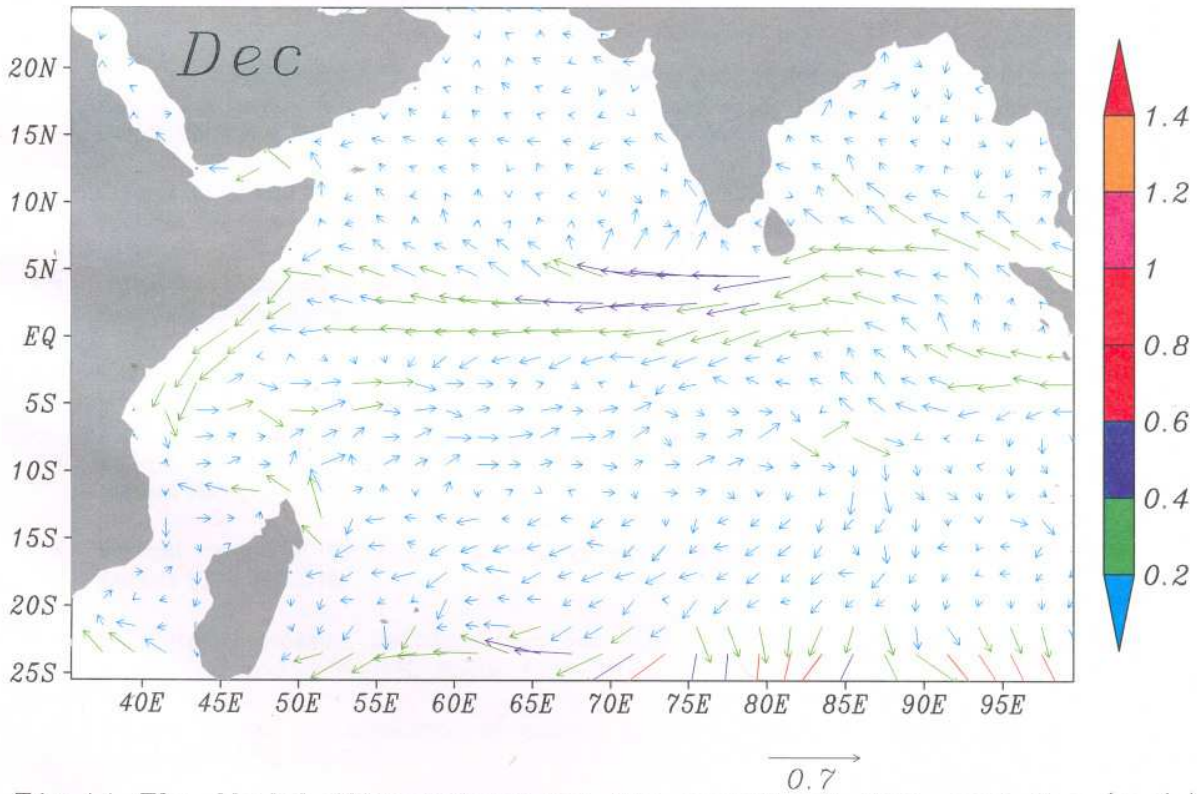

Fig.11 The Model Climatology for the month of Nov. and Dec.(m/s)

I. I. T. M. RESEARCH REPORTS

- Energetic consistency of truncated models, Asnani G.C., August 1971, RR-001.
- Note on the turbulent fluxes of heat and moisture in the boundary layer over the Arabian Sea, Sinha S., August 1971, RR-002.
- Simulation of the spectral characteristics of the lower atmosphere by a simple electrical model and using it for prediction, Sinha S., September 1971, RR-003.
- Study of potential evapo-transpiration over Andhra Pradesh, Rakhecha P.R., September 1971, RR-004.
- Climatic cycles in India-1: Rainfall, Jagannathan P. and Parthasarathy B., November 1971, RR-005.
- Tibetan anticyclone and tropical easterly jet, Raghavan K., September 1972, RR-006.
- Theoretical study of mountain waves in Assam, De U.S., February 1973, RR-007.
- Local fallout of radioactive debris from nuclear explosion in a monsoon atmosphere, Saha K.R. and Sinha S., December 1972, RR-008.
- Mechanism for growth of tropical disturbances, Asnani G.C. and Keshavamurty R.N., April 1973, RR-009.
- Note on "Applicability of quasi-geostrophic barotropic model in the tropics", Asnani G.C., February 1973, RR-010.
- On the behaviour of the 24-hour pressure tendency oscillations on the surface of the earth, Part-I: Frequency analysis, Part-II: Spectrum analysis for tropical stations, Misra B.M., December 1973, RR-011.
- On the behaviour of the 24 hour pressure tendency oscillations on the surface of the earth, Part-III : Spectrum analysis for the extra-tropical stations, Misra B.M., July 1976, RR-011A.
- Dynamical parameters derived from analytical functions representing Indian monsoon flow, Awade S.T. and Asnani G.C., November 1973, RR-012.
- Meridional circulation in summer monsoon of Southeast Asia, Asnani G.C., November 1973, RR-014.
- Energy conversions during weak monsoon, Keshavamurty R.N. and Awade S.T., August 1974, RR-015.
- Vertical motion in the Indian summer monsoon, Awade S.T. and Keshavamurty R.N., August 1974, RR-016.
- Semi-annual pressure oscillation from sea level to 100mb in the northernhemisphere, Asnani G.C. and Verma R.K., August 1974, RR-017.
- Suitable tables for application of gamma probability model to rainfall, Mooley D.A., November 1974, RR-018.
- Annual and semi-annual thickness oscillation in thenorthern hemisphere, Asnani G.C. and Verma R.K., January 1975, RR-020.

- Spherical harmonic analysis of the normal constant pressure charts in the northern hemisphere, Awade S.T., Asnani G.C. and Keshavamurty R.N., May 1978, RR-021.
- Dynamical parameters derived from analytical function representing normal July zonal flow along 87.5 °E, Awade S.T. and Asnani G.C., May 1978, RR-022.
- Study of trends and periodicities in the seasonal and annual rainfall of India, Parthasarathy B. and Dhar O.N., July 1975, RR-023.
- Southern hemisphere influence on Indian rainfall, Raghavan K.., Paul D.K. and Upasani P.U., February 1976, RR-024.
- Climatic fluctuations over Indian region - Rainfall : A review, Parthasarathy B. and Dhar O.N., May 1978, RR-025.
- Annual variation of meridional flux of sensible heat, Verma R.K. and Asnani G.C., December 1978, RR-026.
- Poisson distribution and years of bad monsoon over India, Mooley D.A and Parthasarathy B., April 1980, RR-027.
- On accelerating the FFT of Cooley and Tukey, Mishra S.K., February 1981, RR-028.
- Wind tunnel for simulation studies of the atmospheric boundary layer, Sivaramakrishnan S., February 1981, RR-029.
- Hundred years of Karnataka rainfall, Parthasarathy B. and Mooley D.A., March 1981, RR-030.
- Study of the anomalous thermal and wind patterns during early summer season of 1979 over the Afro-Asian region in relation to the large-scale performance of the monsoon over India, Verma R.K. and Sikka D.R., March 1981, RR-031.
- Some aspects of oceanic ITCZ and its disturbances during the onset and established phase of summer monsoon studied with Monex-79 data, Sikka D.R., Paul D.K. and Singh S.V., March 1981, RR- 032.
- Modification of Palmer drought index, Bhalme H.N. and Mooley D.A., March 1981, RR-033.
- Meteorological rocket payload for Menaka-II/Rohini 200 and its developmental details, Vernekar K.G. and Brij Mohan, April 1981, RR-034.
- Harmonic analysis of normal pentad rainfall of Indian stations, Anathakrishnan R. and Pathan J.M., October 1981, RR-035.
- Pentad rainfall charts and space-time variations of rainfall over India and the adjoining areas, Anathakrishnan R. and Pathan J.M., November 1981, RR-036.
- Dynamic effects of orography on the large scale motion of the atmosphere Part I : Zonal flow and elliptic barrier with maximum height of one km., Bavadekar S.N. and Khaladkar R.M., January 1983, RR-037.
- Limited area five level primitive equation model, Singh S.S., February 1983, RR-038.
- Developmental details of vortex and other aircraft thermometers, Vernekar K.G., Brij Mohan and Srivastava S., November 1983, RR-039.
- Note on the preliminary results of integration of a five level P.E. model with westerly wind and low orography, Bavadekar S.N., Khaladkar R.M., Bandyopadhyay A. and Seetaramayya P., November 1983, RR-040.

- Long-term variability of summer monsoon and climatic change, Verma R.K., Subramaniam K. and Dugam S.S., December 1984, RR-041.

- Project report on multidimensional initialization for NWP models, Sinha S., February 1989, RR-042.

- Numerical experiments with inclusion of orography in five level P.E. Model in pressure-coordinates for interhemispheric region, Bavadekar S.N. and Khaladkar R.M., March 1989, RR-043.

- Application of a quasi-lagrangian regional model for monsoon prediction, Singh S.S. and Bandyopadhyay A., July 1990, RR-044.

- High resolution UV-visible spectrometer for atmospheric studies, Bose S., Trimbake H.N., Londhe A.L. and Jadhav D.B., January 1991, RR-045.

- Fortran-77algorithm for cubic spline interpolation for regular and irregular grids, Tandon M.K., November 1991, RR-046.

- Fortran algorithm for 2-dimensional harmonic analysis, Tandon M.K., November 1991, RR- 047.

- 500 hPa ridge and Indian summer monsoon rainfall : A detailed diagnostic study, Krishna Kumar K., Rupa Kumar K. and Pant G.B., November 1991, RR-048.

- Documentation of the regional six level primitive equation model, Singh S.S. and Vaidya S.S., February 1992, RR-049.

- Utilisation of magnetic tapes on ND-560 computer system, Kripalani R.H. and Athale S.U., July 1992, RR-050.

- Spatial patterns of Indian summer monsoon rainfall for the period 1871-1990, Kripalani R.H., Kulkarni A.A., Panchawagh N.V. and Singh S.V., August 1992, RR-051.

- FORTRAN algorithm for divergent and rotational wind fields, Tandon M.K., November 1992, RR-052.

- Construction and analysis of all-India summer monsoon rainfall series for the longest instrumental period: 1813-1991, Sontakke N.A., Pant G.B. and Singh N., October 1992, RR-053.

- Some aspects of solar radiation, Tandon M.K., February 1993, RR-054.

- Design of a stepper motor driver circuit for use in the moving platform, Dharmaraj T. and Vernekar K.G., July 1993, RR-055.

- Experimental set-up to estimate the heat budget near the land surface interface, Vernekar K.G., Saxena S., Pillai J.S., Murthy B.S., Dharmaraj T. and Brij Mohan, July 1993, RR-056.

- Identification of self-organized criticality in atmospheric total ozone variability, Selvam A.M. and Radhamani M., July 1993, RR-057.

- Deterministic chaos and numerical weather prediction, Selvam A.M., February 1994, RR-058.

- Evaluation of a limited area model forecasts, Singh S.S., Vaidya S.S Bandyopadhyay A., Kulkarni A.A, Bawiskar S.M.,Sanjay J., Trivedi D.K. and Iyer U., October 1994, RR-059.

- Signatures of a universal spectrum for atmospheric interannual variability in COADS temperature time series, Selvam A.M., Joshi R.R. and Vijayakumar R., October 1994, RR-060.

- Identification of self-organized criticality in the interannual veriability of global surface temperature, Selvam A.M. and Radhamani M., October 1994, RR-061.
- Identification of a universal spectrum for nonlinear veriability of solar-geophysical parameters, Selvam A.M., Kulkarni M.K., Pethkar J.S. and Vijayakumar R., October 1994, RR-062.
- Universal spectrum for fluxes of energetic charged particles from the earth's magnetosphere, Selvam A.M. and Radhamani M., June 1995, RR-063.
- Estimation of nonlinear kinetic energy exchanges into individual triad interactions in the frequency domain by use of the cross-spectral technique, Chakraborty D.R., August 1995, RR-064.
- Monthly and seasonal rainfall series for all-India homogeneous regions and meteorological subdivisions: 1871-1994, Parthasarathy B., Munot A.A. and Kothawale D.R., August 1995, RR-065.
- Thermodynamics of the mixing processes in the atmospheric boundary layer over Pune during summer monsoon season, Morwal S.B. and Parasnis S.S., March 1996, RR-066.
- Instrumental period rainfall series of the Indian region: A documentation, Singh N. and Sontakke N.A., March 1996, RR-067.
- Some numerical experiments on roundoff-error growth in finite precision numerical computation, Fadnavis S., May 1996, RR-068.
- Fractal nature of MONTBLEX time series data, Selvam A.M. and Sapre V.V., May 1996, RR-069.
- Homogeneous regional summer monsoon rainfall over India: Interannual variability and teleconnections, Parthasarathy B., Rupa Kumar K. and Munot A.A., May 1996, RR-070.
- Universal spectrum for sunspot number variability, Selvam A.M. and Radhamani M., November 1996, RR-071.
- Development of simple reduced gravity ocean model for the study of upper north Indian Ocean, Behera S.K. and Salvekar P.S., November 1996, RR-072.
- Study of circadian rhythm and meteorological factors influencing acute myocardial infraction, Selvam A.M., Sen D. and Mody S.M.S., April 1997, RR-073.
- Signatures of universal spectrum for atmospheric gravity waves in southern oscillation index time series, Selvam A.M., Kulkarni M.K., Pethkar J.S. and Vijayakumar R., December 1997, RR-074.
- Some example of X-Y plots on Silicon Graphics, Selvam A.M., Fadnavis S. and Gharge S.P., May 1998, RR-075.
- Simulation of monsoon transient disturbances in a GCM, Ashok K., Soman M.K. and Satyan V.,August 1998, RR-076.
- Universal spectrum for intraseasonal variability in TOGA temperature time series, Selvam A.M., Radhamani M., Fadnavis S. and Tinmaker M.I.R., August 1998, RR-077.
- One dimensional model of atmospheric boundary layer, Parasnis S.S., Kulkarni M.K., Arulraj S. and Vernekar K.G., February 1999, RR-078.
- Diagnostic model of the surface boundary layer - A new approach, Sinha S., February 1999, RR-079.
- Computation of thermal properties of surface soil from energy balance equation using force - restore method, Sinha S., February 1999, RR-080.

- Fractal nature of TOGA temperature time series, Selvam A.M. and Sapre V.V., February 1999, RR-081.

- Evolution of convective boundary layer over the Deccan Plateau during summer monsoon, Parasnis S.S., February 1999, RR-082.

- Self-organized criticality in daily incidence of acute myocardial infarction, Selvam A.M., Sen D., and Mody S.M.S., Feburary 1999, RR-083.

- Monsoon simulation of 1991 and 1994 by GCM : Sensitivity to SST distribution, Ashrit R.G., Mandke S.K. and Soman M.K., March 1999, RR-084.

- Numerical investigation on wind induced interannual variability of the north Indian Ocean SST, Behera S.K., Salvekar P.S. and Ganer D.W., April 1999, RR-085.

- On step mountain eta model, Mukhopadhyay P., Vaidya S.S., Sanjay J. and Singh S.S., October 1999, RR-086.

- Land surface processes experiment in the Sabarmati river basin: an overview and early results, Vernekar K.G., Sinha S., Sadani L.K., Sivaramakrishnan S., Parasnis S.S., Brij Mohan, Saxena S., Dharamraj T., Pillai, J.S., Murthy B.S., Debaje, S.B., Patil, M.N. and Singh A.B., November 1999, RR-087.

- Reduction of AGCM systematic error by Artificial Neural Network: A new approach for dynamical seasonal prediction of Indian summer monsoon rainfall, Sahai A.K. and Satyan V., December 2000, RR-088.

- Ensemble GCM simulations of the contrasting Indian summer monsoons of the 1987 and 1988, Mujumdar M. and Krishnan R., February 2001, RR-089.

- Aerosol measurements using lidar and radiometers at Pune during INDOEX field phases, Maheskumar R.S., Devara P.C.S., Raj P.E., Jaya Rao Y., Pandithurai G., Dani K.K., Saha S.K., Sonbawne S.M. and Tiwari Y.K., December 2001, RR-090.

- Modelling studies of the 2000 Indian summer monsoon and extended analysis, Krishnan R., Mujumdar M., Vaidya V., Ramesh K.V. and Satyan V., December 2001, RR-091.

- Intercomparison of Asian summer monsoon 1997 simulated by atmospheric general circulation models, Mandke S.K., Ramesh K.V. and Satyan V., December 2001, RR-092.

- Prospects of prediction of Indian summer monsoon rainfall using global SST anomalies, Sahai A.K, Grimm A.M., Satyan V. and Pant G.B., April 2002, RR-093.

- Estimation of nonlinear heat and momentum transfer in the frequency domain buy the use of frequency co-spectra and cross-bispectra, Chakraborty D.R. and Biswas M.K., August 2002, RR-094

- Real time simulations of surface circulations by a simple ocean model, Reddy P.R.C., Salvekar P.S., Ganer D.W. and Deo A.A., January 2003, RR-095

- Evidence of twin gyres in the Indian ocean : new insights using reduced gravity model by daily winds, Reddy P.R.C., Salvekar P.S., Ganer D.W. and Deo A.A., February 2003, RR-096

- Dynamical seasonal prediction experiments of the Indian summer monsoon, Mujumdar M., Krishnan R. and Satyan V., June 2003, RR-097

- Thermodynamics and dynamics of the upper ocean mixed layer in the central and eastern Arabian Sea, Gnanaseelan C., Mishra A.K., Thompson B.and. Salvekar P.S, August 2003, RR-098

- Measurement of profiles and surface energy fluxes on the west coast of India at Vasco-Da-Gama, Goa during ARMEX 2002-03, Sivaramakrishnan S., Murthy B.S., Dharamraj T., Sukumaran C.and Rajitha Madhu Priya T., August 2003, RR-099

- Time – mean oceanic response and interannual variability in a global ocean GCM simulation, Ramesh K.V. and Krishnan R., September 2003, RR-100

- Multimodel scheme for prediction of monthly rainfall over India, Kulkarni J.R., Kulkarni S.G., Badhe Y., Tambe S S.., Kulkarni B.D. and Pant G.B., December 2003, RR-101

- Mixed layer and thermocline interactions associated with monsoonal forcing over the Arabian Sea, Krishnan R. and Ramesh K.V., January 2004, RR-102

- Interannual variability of Kelvin and Rossby waves in the Indian Ocean from TOPEX/ POXEIDON altimetry data, Gnanaseelan C., Vaid B.H., Polito P.S. and Salvekar P.S., March 2004, RR-103

- Initialization experiments over Indian region with a limited area model using recursive digital filters, Badyopadhyay S. and Mahapatra S., July 2004, RR-104

- Sensitivity of Indian monsoon rainfall to different convective parameters in the relaxed Arakawa-Schubert scheme, Pattanaik D.R. and Satyan V., October 2004, RR-105